The Application of Deep Learning for Classification of Alzheimer's Disease Stages by Magnetic Resonance Imaging Data

Muhammad Irfan[1]*, Seyed Shahrestani[1], Mahmoud ElKhodr[2]

[1] School of Computer, Data and Mathematical Sciences, Western Sydney University, Sydney (Australia)
[2] School of Engineering and Technology, Central Queensland University, Sydney (Australia)

* Corresponding author: 19918600@student.westernsydney.edu.au

Received 5 September 2022 | Accepted 14 April 2023 | Published 31 July 2023

Abstract

Detecting Alzheimer's disease (AD) in its early stages is essential for effective management, and screening for Mild Cognitive Impairment (MCI) is common practice. Among many deep learning techniques applied to assess brain structural changes, Magnetic Resonance Imaging (MRI) and Convolutional Neural Networks (CNN) have grabbed research attention because of their excellent efficiency in automated feature learning of a variety of multilayer perceptron. In this study, various CNNs are trained to predict AD on three different views of MRI images, including Sagittal, Transverse, and Coronal views. This research use T1-Weighted MRI data of 3 years composed of 2182 NIFTI files. Each NIFTI file presents a single patient's Sagittal, Transverse, and Coronal views. T1-Weighted MRI images from the ADNI database are first preprocessed to achieve better representation. After MRI preprocessing, large slice numbers require a substantial computational cost during CNN training. To reduce the slice numbers for each view, this research proposes an intelligent probabilistic approach to select slice numbers such that the total computational cost per MRI is minimized. With hyperparameter tuning, batch normalization, and intelligent slice selection and cropping, an accuracy of 90.05% achieve with the Transverse, 82.4% with Sagittal, and 78.5% with Coronal view, respectively. Moreover, the views are stacked together and an accuracy of 92.21% is achived for the combined views. In addition, results are compared with other studies to show the performance of the proposed approach for AD detection.

Keywords

Alzheimer's Disease, ANDI Database, Classification, Cognitive Impairment, Convolutional Neural Network, Deep Learning, Magnetic Resonance Imaging.

DOI: 10.9781/ijimai.2023.07.009

I. Introduction

ALZHEIMER'S Disease (AD) is the most common type of dementia. It is a irreversible, progressive, and chronic neurodegenerative disease starts with mild memory loss and possibly leading to the serious memory loss and even death [1]. AD involves parts of the brain that control thought, memory, and language. It is clinically expressed by cognitive dysfunction, amnesia, and steady loss of various brain functions and everyday living independent actions [2]. AD patients are anticipated to grow worldwide from today's figure of 47 million to 152 million by 2050 [2]. This anticipated increase will produce tremendous medical, social, and economic impacts [3], [4]. AD may cause shrinking in some areas of the human brain, reduce the brain's hippocampal size, and in some cases, lead to an enlargement in the brain ventricles [4]. Additionally, the pathogenesis of AD remains not fully explored, and the available therapies cannot reverse it or completely stop its progression. Mild Cognitive Impairment (MCI) and Cognitive Normal (CN) tests are typically conducted by neurologists to detect AD [5]. However, these tests are challenging and complex. [6]. Studies have shown that most patients who suffer from Mild Cognitive Impairment are at risk of developing Dementia or other forms of AD. About 10–15% of people with MCI progress to AD annually [7].

Detecting AD using MCI screening is critical for successfully designing and implementing care practices and policies to counter disease deterioration. Therefore, early and stages detection is crucial to slow down the progression of the disease as it enables the development of early intervention and treatment plans [8]. Neuropathology changes in the brain help detect AD and its progression. For instance, the brain's gray matter loss has accompanied MCI and AD [6]. Typically, neurologists use clinical methodologies such as Cerebrospinal Fluid (CSF) examinations to classify AD [9]. An increase in the norepinephrine level in the CSF indicates AD progression. The CSF is usually collected directly from the brain ventricles [10]. However, CSF collection and examinations carry risks [11], [12]. Alternatively,

Please cite this article as:
M. Irfan, S. Shahrestani, M. ElKhodr. The Application of Deep Learning for Classification of Alzheimer's Disease Stages by Magnetic Resonance Imaging Data, International Journal of Interactive Multimedia and Artificial Intelligence, vol. 9, no. 2, pp. 18-25, 2025, http://dx.doi.org/10.9781/ijimai.2023.07.009

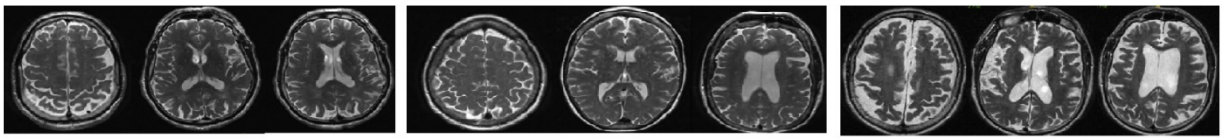

Cognitive Normal (CN) | Mild Cognitive Impairment (MCI) | Alzheimer's Disease (AD)

Fig. 1. Cross-sections from MRI images of CN, MCI, and AD.

non-invasive procedures such as MRI have been used by physicians to determine and assess any changes in the brain. Neurologist uses MRI scans to observe and analyze the structural changes in the brain that might be caused by AD, MCI, and CN manifestation [13]. Therefore, neuroimaging helps in visualizing the structural changes in the brain. Fig. 1 shows the changes in the brain of an AD patient. The ventricle enlargement and the changes in the hippocampal size can be observed in these MRI samples, which were taken from the ANDI database. Fig. 1 shows a comparison between images of an AD brain with cortical atrophy with the MRI images of an MCI and a CN patient. The brain texture changes with the progression of AD disease (CN to MCI to AD). Morphological changes in the texture, volume, and structure of the brain are usually used as indicators of the brain's health [14], [15].

Many studies, such as reported [16]-[26], have used neuroimaging biomarkers to predict the stages or the progress of AD. Commonly, MRI images are extensively used in all these studies due to their high resolutions and reasonable cost. Many successful machine learning frameworks have used MRI to predict AD [27], a few of them including RF (random forests) [28], SVM (support vector machine) [29], and boosting techniques [30]. Current machine learning frameworks generally involve a manual assortment of the defined ROI (regions of interest) of the patient brain based on known MRI feature representation [16]-[26], [31].

However, Manual ROI assortment can be susceptible to subjective errors [30], [32], [33]. A manual and automated ROI assortment comparison is presented in [33]. The findings demonstrate significant differences between manual and automated approaches to ROI analysis. The automated process led to a larger estimated task-related effect size. The percent of activated voxels in the automated approach was also more prominent than that of the manual approach in both lesioned and control brains and the right and left hemispheres [33].

To fill this gap, this study proposes the application of deep learning to extract signifying features from brain MRI images. The proposed method utilizes a four-layered Convolutional Neural Network (CNN) architecture to classify clinically evaluated patients with AD into people with MCI and those who are CN.

A two-dimensional (2D) CNN architecture to detect the different stages of AD is proposed in this work. The labeled data is selected from the ANDI dataset [34] and applied 2D-CNN with preprocessing to improve the detection accuracy. The MRI data to train the CNN has three different labels: AD, MCI, and CN, respectively. This work has considered T1-weighted data files. Each file contains a sagittal, coronal, and transverse view. A sample of the views is shown in Fig. 2. Noise is evident in MRI images. Therefore, preprocessing is first applied to extract the brain parts from these images. A three-layered CNN architecture with two dense layers is implemented to detect AD stages. The preprocessing pipeline in this study includes skull stripping, spatial normalization, smoothing, grey normalization, slicing, and resizing. After tuning the parameters and hyperparameters of the CNN, the prediction accuracies of AD stages are significantly improved. In addition, intelligent frame selection and batch normalization reduced the model overfitting. The main contributions of this study include:

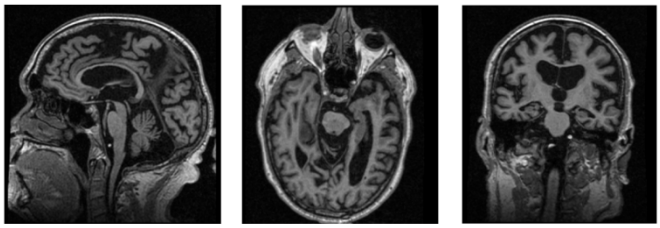

a) Sagittal Slice | b) Coronal Slice | c) Transverse Slice

Fig. 2. Sample views of MRI images from the ADNI database.

- A 2D CNN architecture to detect the different stages of AD is proposed which is trained on the labeled data from ANDI dataset.
- Efficient preprocessing pipeline, slices selection and cropping is proposed to reduce the input data size and avoid model's underfitting.
- The proposed model is trained on three views of MRI, separately and combined.
- A wide set of comparison is performed between different views and the recent state-of-the-art literature.

The remaining of this paper is organized as follows. Section II presents the background of this work and its related studies. Our proposed methodology for classifying AD stages is explained in Section III. Section IV discusses the obtained experimental results and outcomes. Finally, the last section gives the conclusions of this work.

II. Related Studies

Deep learning approaches attempt to imitate the human brain by utilising CNNs, RNNs, stacked auto-encoder, and deep belief networks (DBNs) [35], [36], [37], [38]. They transform low-level features available in the data to build an abstract high-level representation of the learning systems [39]. A dual-tree complex wavelet transform-based method in [40] extracts features from the input, followed by classification with FDNN (feedforward neural network). CNN is a deep multilayer artificial neural network (ANN) composed of convolutional layers, allowing a model to extract feature maps learned from the product of inputs and kernels, thereby detecting the patterns. Moreover, CNNs have shown high accuracy in feature classification [41]-[43]. In the segmentation applications, CNNs outperformed other methodologies such as SVM and logistic regression, which showed less intrinsic feature extraction capabilities [44]. CAD (Computer-Aided Diagnosis) systems built on CNNs successfully detect neurodegenerative diseases [45]. CNN architectures, including the ResNet and GoogleNet, have been successfully used in differentiating the healthy from AD and MCI [46]. LeNet-5 CNN architecture differentiates AD from the NC brain [47]. A deep supervised adaptive 3D-CNN in [48] predicted AD by stacking 3D Convolutional autoencoders without stripping the skull structure. ResNet-152 in [41] obtained highly-discriminative features to detect the stage of the disease progression (AD, MCI, and CN) using neuroimaging data taken from the ADNI database. The study in [49] has used transfer learning and VGG-16 pre-trained architecture for multiclass AD classification on AD, MCI, and CN. The study in [50] implemented 3D-ResNet-18 with data augmented Resnet-18 for feature extraction to classify AD stages accurately. ResNet-18 architecture

was modified in [51] for the binary AD classification: CN vs. AD, CN vs. MCI, AD vs. MCI, and CN vs. MCI. The Transfer Learning scheme is used in [52] for the three-way classification (AD, CN, MCI) of MRI images, implemented in three pre-trained CNNs, including ResNet-18, ResNet-50, and ResNet-101, respectively. A 2D-CNN architecture in [53] used ResNet-50 with diverse activations and batch normalization to classify brain slices into NC, MCI, and AD.

SegNet can classify patients' AD stages using extracted morphological local features from the brain [54]. Resnet-101 also attempted to classify AD, MCI, and CN stages. In [55], A 3D-CNN used a classifier to differentiate the CN and AD using brain MRI images. Using the ADNI dataset, a probability-based CNNs fusion in [47] used DenseNet to detect AD stages. A 3-D Net-121 with a 70% dropout rate is shown to detect the AD stages [56]. A layer-wise Transfer Learning using VGG-19 in [57] discriminated the CN, early MCI, late MCI, and AD. Another Transfer Learning method was presented in [58], which recommended VGG-16 to accurately classify brain MRI slices into CN, MCI, and AD. A pre-trained AlexNet in [59] extracted significant features from the MRI images to classify the AD. Another fine-tuned pre-trained AlexNet, presented in [60] used Transfer Learning to classify the MRI images. In addition, a modified AlexNet in [61] with the parameters adjustment discriminated AD stages. In [62], various pre-trained architectures were utilized after fine-tuning the Transfer Learning approach for CN, MCI, and AD classification from the ADNI dataset. For the AD and MCI prediction, an ensemble of densely-connected 3D-CNNs is suggested in [63] for improving usage of extracted features. The CNN topologies for the binary classification (AD/MCI or MCI/CN) are proposed in [64] by integrating freezing characteristics engaged from ImageNet dataset. Usullay MRI images are used with one or few views without removing the redundant information and noise. In addition, no preprocessing is generally applied for neural networks to learn better. After styding the related research, the issues addressed by preprocessing the MRI images along with noise removal for efficient feature learning. Many denoisiyng methods can be applied such as in [65]-[67].

A 2D CNN architecture to detect different stages of AD is proposed in this work. The CNN architecture is fine-tuned on the dataset, which is preprocessed by a feature engineering method. After parameters and hyperparameters tuning the CNN, AD stages' prediction accuracies are significantly improved. The intelligent frame selection and batch normalization reduced model overfitting. The MRI data to train the CNN has three different labels: AD, MCI, and CN, respectively. This work has considered T1-weighted data files. Each file contains a sagittal, coronal, and transverse view.

III. Methodology

A. Dataset

This study uses the MRI data from the Alzheimer's disease Neuroimaging Initiative (ADNI) database. ADNI is a labeled dataset that has three different labels, i.e., Alzheimer's disease (AD), Mild Cognitive Impairment (MCI), and Cognitive Normal (CN). This dataset contains data about the multiple visits of the same patient during the trial. There are 2182 NIFTI files (3D view MRI images). Each NIFTI file contains a single subject's sagittal, coronal, and transverse views. There is almost 200+ sequenced frames of all three views of the MRI images. Sample views of some of the MRI images taken from the ADNI database are presented in Fig. 2. Since the initial views are noisy and difficult to process, therefore, brain part has been extracted from the MRI to allow further processing. These details of this process are provided in Section B. The dataset distribution gender and label, along with the statistics, age, and the number of visits, are given in Table I.

TABLE I. The Dataset Distribution

Male Patients	1279
Female Patients	930
Cognitive Normal (CN)	748
Mild Cognitive Impairment (MCI)	981
Alzheimer's Disease (AD)	453
Average Age of Patients	76.23
Average Patients Visits	4.10
Age Standard Deviation	6.80

B. MRI Preprocessing

The T1-Weighted MRI data from the ANDI in NIFTI format was preprocessed using the CAT12 toolkit of SPM12 toolbox (MATLAB third party toolbox) with default settings. The preprocessing pipeline includes skull stripping, spatial normalization and smoothing such that after preprocessing, all MRI images follow the dimension (121×145×121), that is (X × Y × Z) with a spatial resolution of (1.5×1.5×1.5) mm3/voxel. In addition, all MRI images, including each voxel value, were normalized in terms of signal intensity. The original value was divided by the actual maximal value of the MRI image. This normalization yields values in the range of 0 and 1. The resultant views after preprocessing the pipeline are shown in Fig. 3. The 3D-MRI (121×145×121), which is the number of sagittal, coronal, and transverse views, were acquired via re-slicing, i.e., (145×121), (121×121), and (121×145), respectively. All the 2D slices were resized to (145×145) after edge padding and zero filling. After resizing, each 2D slice was squared, whereas the central and spatial resolution of the reformatted MRI image remained unchanged.

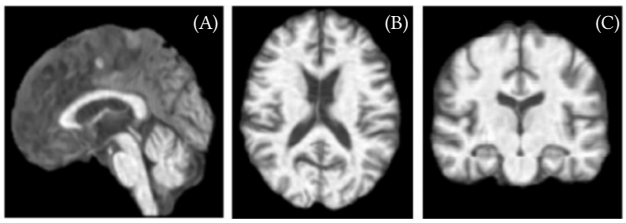

Fig. 3. MRI Preprocessed Views; (A) Sagittal Slice, (B) Coronal Slice, and (C) Transverse Slice.

1. Skull Stripping

A skull stripping method is integral in brain image processing applications [68]. It acts as a preliminary step in numerous medical ML applications as it increases the speed and accuracy of diagnosis manifold [69]. It removes non-cerebral tissues like the skull, scalp, and dura from brain images. Adaptive Probability Region-Growing (APRG) is a method that refines the probability maps by region-growing techniques [64]. This is currently the method with the most accurate and reliable results. This research has removed the skull from MRI data using the APRG method.

2. Spatial Normalization

Human brains differ in size and shape, and one goal of spatial normalization is to deform the human brain scans, so one location in one subject's brain scan corresponds to the same location in another subject's brain scan. More specifically, images from different subjects must be transformed spatially so that they all reside in the same coordinate system, with anatomically corresponding regions being in similar locations. Spatial normalization is a particular form of image registration that maps a subject's MRI image to a reference brain space to allow comparisons across subjects with varied brain morphologies [70]. This research used Diffeomorphic Anatomical Registration Through Exponentiated Lie Algebra (DARTEL) registrations and its existing templates for spatial registration. Furthermore, an optimized

shooting approach is applied that uses an adaptive threshold and lower initial resolutions to obtain a good tradeoff between accuracy and calculation time by selecting the first of the six images (iterations) of a DARTEL template similar to work conducted in [65].

3. Smoothing

Smoothing is used to remove the different noises from the MRI frames. Then, the Gaussian filter is applied to the MRI data to reduce the noise. The images are shown in Fig. 3, which depicts the finalized preprocessed frames of all three views.

C. Proposed Features Engineering

After preprocessing, there are almost 150 slices per view per MRI image. These large numbers of frames require substantial computation power to train a CNN model on them. Moreover, data redundancy would cause the CNN to be overfitting. Therefore, reducing the number of frames of each view is essential to reduce the total computational power needed to process each MRI. To address this challenge, a recent research has randomly selected 40 sagittal slices, 50 coronal slices, and 33 transverse slices, i.e., 123 slices of a subject's 3D brain image [66]. However, the random selection of frames is not convincing as it is unknown which frame contains more information. Random selection can lead to loss of information. To fill this gap, this research relied on a new method that used statistical analysis when selecting the important frames. Firstly, several informative pixels are calculated. If a slice has less than a threshold value of informative pixels, these slices were discarded, and the remaining frames are selected. The formula used for calculating the number of informative pixels is given in (1):

$$I = 1 - \frac{N_0}{H_I \times W_I} \tag{1}$$

Where N_0 is the number of zeros in an image, H_I is the Height of the image, and W_I is the width of the image. This study has selected the highest 40 informative frames of each view, resulting in 120 frames per patient. The process of statistical selection of frames has resulted in reducing the computational complexity of MRI features selection process. Given that every single frame contained various sizes of the informative region. A generic average windows size was calculated for all the patients and all the three views (sagittal, coronal, and transverse) using the proposed algorithm. The subsequent slices have further reduced the computational complexity of the MRI file processing. A sample transverse view after slice cropping is shown in Fig. 4.

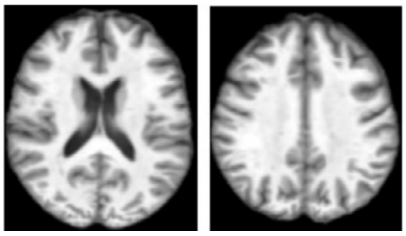

Fig. 4. Sample Transverse View of Slices.

Algorithm for Generic Windows Size

for slice in ISS (Intelligently Selected Slices):
    for patient in patients:
        find top, bottom, left, and right first zero vector
        drop the zero valued vectors from frame
average the cropped image (*windows size*)

D. Convolutional Neural Network (CNN)

The CNN neural model has recently gained significant research attention with remarkable success in recognizing images [42]. The input images move through a chain of convolution layers with CNN, including filtering, pooling, and fully connected dense layers. In addition, the softmax activation function is usually applied for a probabilistic classification of the images between 0 and 1, making CNN appropriate for image feature representation learning. In CNN, a convolution layer contains the extraction and mapping of features. During the feature extraction, all neurons are connected to the local accessible fields of the higher layer for local feature extraction. After the local feature extraction, a spatial relationship with other features is concluded.

On the other hand, convolution operations are applied to the input data using learnable filters (kernels) to produce a feature map during the feature mapping. Multiple feature maps can be computed with a chain of filters. In this manner, the CNN parameters are tuned and can be effectively reduced. After the convolutional layer, the max-pooling layer executes a down-sampling operation in addition to the spatial dimensions. Such a distinctive dual-feature extraction scheme can successfully moderate the feature resolution. The activations usually use nonlinear functions such as the sigmoid, tanh, ReLU, and Leaky ReLU. To accelerate the learning and prevent overfitting of the proposed model, pooling layers were integrated into the CNN. This layer reduces the samples extracted from the data, thereby reducing the spatial information. Average pooling and max-pooling are the prominent pooling schemes. The FC (fully-connected) layer is similar to the Artificial Neural Network (ANN). Its task is to set a path for effective detection. An example demonstration of the CNN model's convolutional, pooling, and fully connected layers are shown in Fig. 5.

This study mainly used CNN with the following architecture to recognize 2D MRI images. The preprocessed MRI image was fed into the CNN model as feature extraction and mapping vectors. Then, the max-pooling layer learns the features from the training data. This process improves the effectiveness of CNN instead of manually extracting the features. The CNN was trained by applying the learnable filters and convolutional operations. Using a local weight distribution has significantly reduced the complexity of the model. The format for CNN with 3D input data follows (Width × Height × No. of Frames). All three views of a single MRI image were treated separately. For each view, an individual CNN was trained. The model architecture for 3D inputs is provided in Table II. The model configurations are provided in Table III.

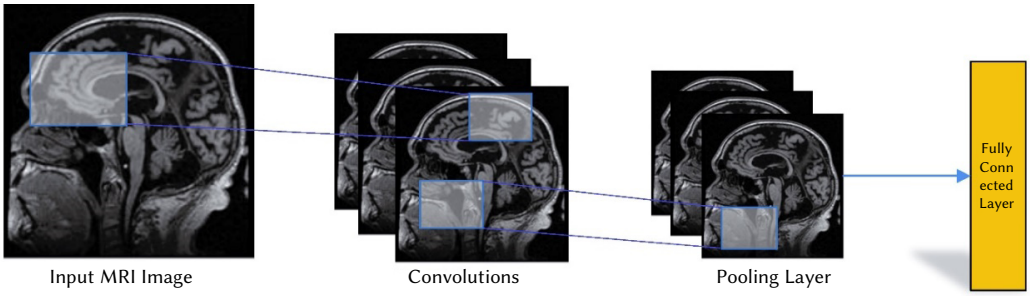

Fig. 5. Example demonstration of the convolutional, pooling, and fully connected layers of the CNN model.

TABLE II. Layers and Parameters in CNN Model for MRI Images

Layers	Output Shape	Para#	Layers	Output Shape	Para#	Layers	Output Shape	Para#
Conv2D	(41, 32, 32)	11552	Conv2D	(13, 10, 64)	18496	Conv2D	(4 3, 128)	73856
L-ReLU	(41, 32, 32)	0	BN	(13, 10, 64)	256	BN	(4 3, 128)	512
			L-ReLU	(13, 10, 64)	0	L-ReLU	(4 3, 128)	0
			Maxpool	(13, 10, 64)	0	Maxpool	(4 3, 128)	0
Flatten Layer: (None, 1536), Para# = 0								
Dense Layer: (None, 100), Para# = 153700								
Dense Layer: (None, 3), Para# = 303								
Total Trainable Para#: 258,291								

(BN= Batch Normalization, Conv2D= 2D Convolution, L-ReLU= Leaky ReLU, Maxpool= Maxpooling layer)

TABLE III. Model Configurations Table

Parameter	Configuration	
Learning Rate	Initial Value	0.001
	Nature	Timely Decreasing (Adaptive)
	Reduction Factor	0.1
	Minimum Possible Value	0.00001
	Reduction Monitoring	Validation Accuracy
	Patient to Reduction	2 times
Stopping Criteria	Stopping Monitoring	Validation Accuracy
	Patience to Stop	20 times
	Initial Learning Rate	0.001
Weights	Trainable	Yes
	Initial Weights	Random
Training	Optimizer	Adam
	Loss	Categorical Cross-Entropy
	Maximum Possible Epochs	Infinite
	Batch Size	32
	Validation Split	15%
	Performance Metric	Accuracy
		Loss

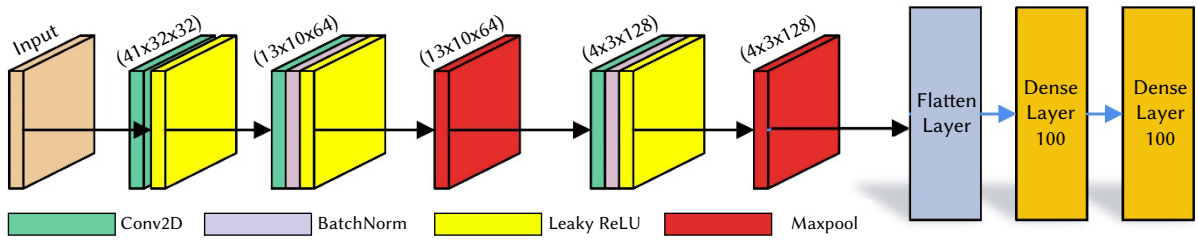

Fig. 6. The architecture of the layers used in the CNN.

The CNN model proposed in this study contains three convolutional layers with different filter numbers, sizes, and strides, two max-pooling layers, and two fully-connected dense layers. Leaky activation and batch normalization are used after the convolutional layers. The architecture of the layers used in the CNN is shown in Fig. 6. The first convolutional layer contains 32 (3×3) size filters and stride 1. Similarly, the second and third convolutional layer contains 64 and 128 filters of size (3×3) and stride 1. All pooling layers use a max-pooling scheme with the pooling window size of (2×2) and strides 2. The last max-pooling layer's output is passed through the flattening layer and converted 2D data into 1D. The output of the flattened layer is fed to the fully-connected dense layer with 100 neurons using softmax as the activation function. The fully-connected layer is an Artificial Neural Network (ANN) based- architecture. ADAptive Moment (ADAM) estimation is used to optimize the learning weights of model, which is extended version of stochastic gradient decent [68]. The learning rate and momentum are fixed to 0.0001, 0.9, and the binary cross-entropy loss function in the CNN model training. If validation accuracy is not improving and patience to stop reaches to maximum point, the model stops at that point, as provided in Table III.

IV. Experimental Results and Discussions

The intelligent frames selection dropped the initial frames with more than 50% zeros. After intelligent frame selection, the frames were normalized between 0 and 1. Finally, the preprocessed data is trained and tested on the same CNN model (as explained in section 3.3). The methodology includes three different strategies. Firstly, different MRI views were trained on the same CNN. This research first presents transverse slices' results where the input frame size was (123×98). Initially, an accuracy of 80.21% is achieved with the transverse view. However, after tuning the parameters and hyperparameters of CNN

model, the prediction accuracy improved from 80.21% to 90.5±1.5%. In addition, an intelligent frame selection and batch normalization reduced the model overfitting. Also, a precision of 87.2±1.2%, Recall with 90.7±1%, and F1 with 90.7±1% F1 measures are achieved with transverse views. Secondly, the results of the sagittal slices where the input frame size to CNN was (106×123) were noted. With the proposed probability-based frame selection and features engineering, the achieved accuracy was 80.5±2.5% for sagittal views.

Moreover, other measures achieved are precision of 80.5±2.5%, Recall with 82.3±2.7%, and F1 score with 81.5±3.1%. Lastly, the results of the coronal slices, where the input frame size was (104×97), were compiled with intelligent frame selection and feature engineering. It achieved an accuracy of 78.5±4.5% for the coronal views. Table IV shows the performance measures in terms of accuracy, precision, recall, and F1 scores for three MRI views, sagittal, coronal, and transverse, respectively. The results indicate that better performance was achieved with transverse views, and the accuracy has improved from 78.5 ± 4.5% to 90.5 ± 1.5%, whereas precision improved from 80.5 ± 2.5% to 87.2 ± 1.2%. This research work has combined all views and trained the same CNN architecture. With this strategy, an accuracy of 92.21% has been achieved. Table V shows all the corresponding measures for the three combined views. The CNN model has been trained and validated for 50 epochs and achieved 90.41% testing accuracy on transverse view.

TABLE IV. CNN's Performance Analysis for Three Separate Views

View	Transverse	Sagittal	Coronal
Accuracy	90.5 ± 1.5	82.4 ± 2.9	78.5 ± 4.5
Precision	87.2 ± 1.2	80.5 ± 2.5	77.3 ± 3.3
Recall	90.7 ± 1	82.3 ± 2.7	79.1 ± 2.8
F1-score	90 ± 1.3	81.5 ± 3.1	77.8 ± 3.1

TABLE V. Performance Analysis of CNN Trained on All Views

Combined Views			
Accuracy	Precision	Recall	F1-Score
92.21 ± 1	89.47 ± 1.3	91.05 ± 2.7	90.25 ± 3.1

Additionally, to further evaluate the performance of the proposed CNN model, the model with frame selection was compared with the PCA+SVM [71], 3D-SENet and CNN+EL 3D-SENet [66]. As a central element of CNN, the convolution operation enables networks to obtain informative feature representation by combining spatial and channel-wise information within local fields. The results in terms of the accuracy of the different models are given in Table VI. It can be observed that CNN with the proposed probabilistic frame selection for early AD detection is more accurate and robust than the PCA+SVM, 3D-SENet, and CNN+EL. The model's accuracy improved from (71.33 ± 0.29)% with PCA+SVM to (83.33 ± 2.96) % with the proposed approach. Also, the accuracy is increased from (75.11 ± 0.23)% and (75.11 ± 0.60) % with 3D-SENet and CNN+EL to (83.33 ± 2.96)% with the proposed model.

TABLE VI. Performance of the Proposed CNN With Other Models

Models	Accuracy of Models
PCA+SVM	71.33 ± 0.29
CNN+EL	75.11 ± 0.60
3D-SENet	75.11 ± 0.23
Proposed	83.33 ± 2.96

The transfer learning with pre-trained models, such as the AlexNet, VGG, and GoogleNet, was also examined against the proposed approach. Most of the classification-prediction problems in medical imaging have been implemented with SVM. Table VII compares the SVM and other models to investigate the performance. The trained model was the most convenient tool for the AD detection prediction problem based on classification accuracy and prediction responses. The SVM classifier presented the result with (70~80) % accuracy. However, CNN models provide a prediction accuracy of (80~90) %, as represented in Fig. 7.

TABLE VII. Performance Analysis of the Proposed CNN With State-of-the-Art Models

Models	Accuracy of Models
Deep learning using AlexNet	85.14%
Deep learning using VGG16	88.92%
Deep learning using VGG19	90.02%
Deep learning using GoogLeNet	87.29%
Support Vector Machine (SVM)	74.25%
Proposed	92.21 ± 2.96

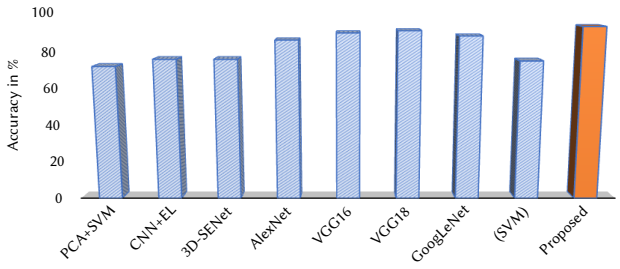

Fig. 7. Overall Accuracy of SVM and CNN-basedModels.

V. Conclusions

This research aimed to deploy unconventional deep learning methods to determine whether they can extract helpful Alzheimer's disease biomarkers from Magnetic Resonance Imaging and classify brain images into Alzheimer's disease, Mild Cognitive Impairment, and Normal Cognitive groups. The T1-Weighted MRI data from the ANDI database in NIFTI format was preprocessed, but many MRI slices required a massive computational cost. Therefore, it was essential to reduce the slice numbers for three MRI views to minimize the total computational cost. Probabilistic frame selection was proposed to address the problem, which has improved the overall CNN accuracy from 80.21% to 90.5±1.5. This study first trained CNNs on three different MRI views (transverse, sagittal, and coronal). During this set of experiments, the proposed approach achieved a better accuracy of (90.5 ± 1.5) and a precision of (87.2 ± 1.2) for transverse views.

Furthermore, all three views were combined and tested with CNN using MRI scans. This proposed approach improved the performance and achieved (92.21 ± 1) accuracy and (89.47 ± 1.3) precision. With intelligent frame selection, the trained CNN model achieved an accuracy of 92.21%, which is significantly better than similar models. It is observed that the absolute accuracy has increased from 71.33% (PCA+SVM), 75.11% (CNN+EL), and 75.11% (3D-SDNet) to 83.33% with the proposed CNN approach. The transfer learning with pre-trained models, such as the AlexNet, VGG, and GoogleNet, was also examined. The CNN models obtained the results in terms of accuracy of (80~90) %, which is higher than SVM classifier, which produced results with an accuracy of (70~80) %. The end-to-end implementation of CNN to classify AD, MCI, and CN groups in three different MRI views reflects the identification of distinctive elements in brain images. In this context, the proposed approach represents a promising tool in finding the biomarkers helping the early AD detection, eventually taking critical and successful care policies to counter deterioration in the disease.

This study includes on T1-weighted MRI scans to detect the different stages of AD. Although with such arrangement, the model achieved the state-of-the art results surpassing the related studies, but furher improvements can be achieved if T2-weighted scans are also utilized. In addition, microarray gene expression data can be used to classify the disease.

References

[1] M. G. Ulep, S. K. Saraon, and S. McLea, "Alzheimer disease," The Journal for Nurse Practitioners, vol. 14, pp. 129-135, 2018.

[2] C. Patterson, "World Alzheimer report 2018," 2018.

[3] J. Wiley, "Alzheimer's disease facts and figures," Alzheimers Dement, vol. 17, pp. 327-406, 2021.

[4] A. Fahimi, M. Noroozi, & A. Salehi, (2021). Enlargement of early endosomes and traffic jam in basal forebrain cholinergic neurons in Alzheimer's disease. Handbook of Clinical Neurology, 179, 207-218.

[5] J. C. Morris and J. L. Price, "Pathologic correlates of nondemented aging, mild cognitive impairment, and early-stage Alzheimer's disease," Journal of Molecular Neuroscience, vol. 17, pp. 101-118, 2001.

[6] S. Liu, S. Liu, W. Cai, S. Pujol, R. Kikinis, and D. Feng, "Early diagnosis of Alzheimer's disease with deep learning," in 2014 IEEE 11th international symposium on biomedical imaging (ISBI), 2014, pp. 1015-1018.

[7] S. Afzal, M. Maqsood, U. Khan, I. Mehmood, H. Nawaz, F. Aadil & Y. Nam, "Alzheimer Disease Detection Techniques and Methods: A Review," International Journal of Interactive Multimedia and Artificial Intelligence, vol. 6, pp. 26-39, 2021.

[8] G. Karas, P. Scheltens, S. A. Rombouts, P. J. Visser, R. A. van Schijndel, N. C. Fox, et al., "Global and local gray matter loss in mild cognitive impairment and Alzheimer's disease," Neuroimage, vol. 23, pp. 708-716, 2004.

[9] K. Blennow, "Cerebrospinal fluid protein biomarkers for Alzheimer's disease," NeuroRx, vol. 1, pp. 213-225, 2004.

[10] R. Elrod, E. R. Peskind, L. DiGiacomo, K. I. Brodkin, R. C. Veith, and M. A. Raskind, "Effects of Alzheimer's disease severity on cerebrospinal fluid norepinephrine concentration," The American journal of psychiatry, vol. 154, pp. 25-30, 1997.

[11] O. Hansson, S. Lehmann, M. Otto, H. Zetterberg, and P. Lewczuk, "Advantages and disadvantages of the use of the CSF Amyloid β (Aβ) 42/40 ratio in the diagnosis of Alzheimer's Disease," Alzheimer's research & therapy, vol. 11, pp. 1-15, 2019.

[12] S. Das and S. Basu, "Multi-targeting strategies for Alzheimer's disease therapeutics: pros and cons," Current Topics in Medicinal Chemistry, vol. 17, pp. 3017-3061, 2017.

[13] S. J. Teipel, M. Grothe, S. Lista, N. Toschi, F. G. Garaci, and H. Hampel, "Relevance of magnetic resonance imaging for early detection and diagnosis of Alzheimer disease," Medical Clinics, vol. 97, pp. 399-424, 2013.

[14] G. H. Weissberger, J. V. Strong, K. B. Stefanidis, M. J. Summers, M. W. Bondi, and N. H. Stricker, "Diagnostic accuracy of memory measures in Alzheimer's dementia and mild cognitive impairment: a systematic review and meta-analysis," Neuropsychology review, vol. 27, pp. 354-388, 2017.

[15] S. Lorio, F. Kherif, A. Ruef, L. Melie-Garcia, R. Frackowiak, J. Ashburner, et al., "Neurobiological origin of spurious brain morphological changes: A quantitative MRI study," Human brain mapping, vol. 37, pp. 1801-1815, 2016.

[16] R. Cuingnet, E. Gerardin, J. Tessieras, G. Auzias, S. Lehéricy, M.-O. Habert, et al., "Automatic classification of patients with Alzheimer's disease from structural MRI: a comparison of ten methods using the ADNI database," neuroimage, vol. 56, pp. 766-781, 2011.

[17] D. Zhang, Y. Wang, L. Zhou, H. Yuan, D. Shen, and A. s. D. N. Initiative, "Multimodal classification of Alzheimer's disease and mild cognitive impairment," Neuroimage, vol. 55, pp. 856-867, 2011.

[18] T. Tong, Q. Gao, R. Guerrero, C. Ledig, L. Chen, D. Rueckert, et al., "A novel grading biomarker for the prediction of conversion from mild cognitive impairment to Alzheimer's disease," IEEE Transactions on Biomedical Engineering, vol. 64, pp. 155-165, 2016.

[19] T. Tong, R. Wolz, Q. Gao, R. Guerrero, J. V. Hajnal, D. Rueckert, et al., "Multiple instance learning for classification of dementia in brain MRI," Medical image analysis, vol. 18, pp. 808-818, 2014.

[20] R. Guerrero, R. Wolz, A. Rao, D. Rueckert, and A. s. D. N. Initiative, "Manifold population modeling as a neuro-imaging biomarker: application to ADNI and ADNI-GO," NeuroImage, vol. 94, pp. 275-286, 2014.

[21] H.-I. Suk, S.-W. Lee, D. Shen, and A. s. D. N. Initiative, "Hierarchical feature representation and multimodal fusion with deep learning for AD/MCI diagnosis," NeuroImage, vol. 101, pp. 569-582, 2014.

[22] B. Cheng, M. Liu, D. Zhang, B. C. Munsell, and D. Shen, "Domain transfer learning for MCI conversion prediction," IEEE Transactions on Biomedical Engineering, vol. 62, pp. 1805-1817, 2015.

[23] S. F. Eskildsen, P. Coupé, V. S. Fonov, J. C. Pruessner, D. L. Collins, and A. s. D. N. Initiative, "Structural imaging biomarkers of Alzheimer's disease: predicting disease progression," Neurobiology of aging, vol. 36, pp. S23-S31, 2015.

[24] F. Li, L. Tran, K.-H. Thung, S. Ji, D. Shen, and J. Li, "A robust deep model for improved classification of AD/MCI patients," IEEE journal of biomedical and health informatics, vol. 19, pp. 1610-1616, 2015.

[25] S. Liu, S. Liu, W. Cai, H. Che, S. Pujol, R. Kikinis, et al., "Multimodal neuroimaging feature learning for multiclass diagnosis of Alzheimer's disease," IEEE Transactions on Biomedical Engineering, vol. 62, pp. 1132-1140, 2014.

[26] E. Moradi, A. Pepe, C. Gaser, H. Huttunen, J. Tohka, and A. s. D. N. Initiative, "Machine learning framework for early MRI-based Alzheimer's conversion prediction in MCI subjects," Neuroimage, vol. 104, pp. 398-412, 2015.

[27] J. M. Mateos-Pérez, M. Dadar, M. Lacalle-Aurioles, Y. Iturria-Medina, Y. Zeighami, and A. C. Evans, "Structural neuroimaging as clinical predictor: A review of machine learning applications," NeuroImage: Clinical, vol. 20, pp. 506-522, 2018.

[28] E. E. Tripoliti, D. I. Fotiadis, and M. Argyropoulou, "A supervised method to assist the diagnosis and monitor progression of Alzheimer's disease using data from an fMRI experiment," Artificial intelligence in medicine, vol. 53, pp. 35-45, 2011.

[29] K. Van Leemput, F. Maes, D. Vandermeulen, and P. Suetens, "Automated model-based tissue classification of MR images of the brain," IEEE transactions on medical imaging, vol. 18, pp. 897-908, 1999.

[30] C. Hinrichs, V. Singh, L. Mukherjee, G. Xu, M. K. Chung, S. C. Johnson, et al., "Spatially augmented LPboosting for AD classification with evaluations on the ADNI dataset," Neuroimage, vol. 48, pp. 138-149, 2009.

[31] N. Arunkumar, M. A. Mohammed, S. A. Mostafa, D. A. Ibrahim, J. J. Rodrigues, and V. H. C. de Albuquerque, "Fully automatic model-based segmentation and classification approach for MRI brain tumor using artificial neural networks," Concurrency and Computation: Practice and Experience, vol. 32, p. e4962, 2020.

[32] F. Li, M. Liu, and A. s. D. N. Initiative, "Alzheimer's disease diagnosis based on multiple cluster dense convolutional networks," Computerized Medical Imaging and Graphics, vol. 70, pp. 101-110, 2018.

[33] K. A. Garrison, C. Rogalsky, T. Sheng, B. Liu, H. Damasio, C. J. Winstein, et al., "Functional MRI preprocessing in lesioned brains: manual versus automated region of interest analysis," Frontiers in Neurology, vol. 6, p. 196, 2015.

[34] N. R. de Vent, J. A. Agelink van Rentergem, B. A. Schmand, J. M. Murre, A. Consortium, and H. M. Huizenga, "Advanced Neuropsychological Diagnostics Infrastructure (ANDI): A normative database created from control datasets," Frontiers in Psychology, vol. 7, p. 1601, 2016.

[35] Y. LeCun, "LeNet-5, convolutional neural networks," URL: http://yann. lecun. com/exdb/lenet, vol. 20, p. 14, 2015.

[36] P. Vincent, H. Larochelle, I. Lajoie, Y. Bengio, P.-A. Manzagol, and L. Bottou, "Stacked denoising autoencoders: Learning useful representations in a deep network with a local denoising criterion," Journal of machine learning research, vol. 11, 2010.

[37] G. E. Hinton, "Deep belief networks," Scholarpedia, vol. 4, p. 5947, 2009.

[38] Z.-J. Sun, L. Xue, Y.-M. Xu, and Z. Wang, "Overview of deep learning," Jisuanji Yingyong Yanjiu, vol. 29, pp. 2806-2810, 2012.

[39] M. Sharma, P. Sharma, R. B. Pachori, and U. R. Acharya, "Dual-tree complex wavelet transform-based features for automated alcoholism identification," International Journal of Fuzzy Systems, vol. 20, pp. 1297-1308, 2018.

[40] A. Farooq, S. Anwar, M. Awais, and S. Rehman, "A deep CNN based multiclass classification of Alzheimer's disease using MRI," in 2017 IEEE International Conference on Imaging systems and techniques (IST), 2017, pp. 1-6.

[41] C. Haarburger, M. Baumgartner, D. Truhn, M. Broeckmann, H. Schneider, S. Schrading, et al., "Multi scale curriculum CNN for context-aware breast MRI malignancy classification," in International Conference on Medical Image Computing and Computer-Assisted Intervention, 2019, pp. 495-503.

[42] B. Khagi and G.-R. Kwon, "3D CNN design for the classification of Alzheimer's disease using brain MRI and PET," IEEE Access, vol. 8, pp. 217830-217847, 2020.

[43] S. Deepak and P. Ameer, "Automated categorization of brain tumor from mri using cnn features and svm," Journal of Ambient Intelligence and Humanized Computing, vol. 12, pp. 8357-8369, 2021.

[44] A. Shakarami, H. Tarrah, and A. Mahdavi-Hormat, "A CAD system for diagnosing Alzheimer's disease using 2D slices and an improved AlexNet-SVM method," Optik, vol. 212, p. 164237, 2020.

[45] A. Ashraf, S. Naz, S. H. Shirazi, I. Razzak, and M. Parsad, "Deep transfer learning for alzheimer neurological disorder detection," Multimedia Tools and Applications, vol. 80, pp. 30117-30142, 2021.

[46] L. M. Heising and S. Angelopoulos, "Operationalizing fairness in medical AI adoption: Detection of early Alzheimer's Disease with 2D CNN," BMJ Health & Care Informatics, 2022.

[47] Y. Huang, J. Xu, Y. Zhou, T. Tong, X. Zhuang, and A. s. D. N. Initiative, "Diagnosis of Alzheimer's disease via multi-modality 3D convolutional neural network," Frontiers in neuroscience, p. 509, 2019.

[48] D. Ebrahim, A. M. Ali-Eldin, H. E. Moustafa, and H. Arafat, "Alzheimer Disease Early Detection Using Convolutional Neural Networks," in 2020 15th International Conference on Computer Engineering and Systems (ICCES), 2020, pp. 1-6.

[49] A. Ebrahimi, S. Luo, R. Chiong, and A. s. D. N. Initiative, "Deep sequence modelling for Alzheimer's disease detection using MRI," Computers in Biology and Medicine, vol. 134, p. 104537, 2021.

[50] M. Odusami, R. Maskeliūnas, R. Damaševičius, and T. Krilavičius, "Analysis of Features of Alzheimer's Disease: Detection of Early Stage from Functional Brain Changes in Magnetic Resonance Images Using a Finetuned ResNet18 Network," Diagnostics, vol. 11, p. 1071, 2021.

[51] D. Prakash, N. Madusanka, S. Bhattacharjee, C.-H. Kim, H.-G. Park, and H.-K. Choi, "Diagnosing Alzheimer's disease based on multiclass MRI scans using transfer learning techniques," Current medical imaging, vol. 17, pp. 1460-1472, 2021.

[52] K. S. Yadav and K. P. Miyapuram, "A Novel Approach Towards Early Detection of Alzheimer's Disease Using Deep Learning on Magnetic Resonance Images," in International Conference on Brain Informatics, 2021, pp. 486-495.

[53] P. Buvaneswari and R. Gayathri, "Deep learning-based segmentation in classification of Alzheimer's disease," Arabian Journal for Science and Engineering, vol. 46, pp. 5373-5383, 2021.

[54] H. Parmar, B. Nutter, R. Long, S. Antani, and S. Mitra, "Spatiotemporal feature extraction and classification of Alzheimer's disease using deep learning 3D-CNN for fMRI data," Journal of Medical Imaging, vol. 7, p. 056001, 2020.

[55] B. Solano-Rojas, R. Villalón-Fonseca, and G. Marín-Raventós, "Alzheimer's disease early detection using a low cost three-dimensional densenet-121 architecture," in International Conference on Smart Homes and Health Telematics, 2020, pp. 3-15.

[56] A. Mehmood, S. Yang, Z. Feng, M. Wang, A. S. Ahmad, R. Khan, et al., "A transfer learning approach for early diagnosis of Alzheimer's disease on MRI images," Neuroscience, vol. 460, pp. 43-52, 2021.

[57] R. Jain, N. Jain, A. Aggarwal, and D. J. Hemanth, "Convolutional neural network based Alzheimer's disease classification from magnetic resonance brain images," Cognitive Systems Research, vol. 57, pp. 147-159, 2019.

[58] F.-P. An, "Medical image classification algorithm based on weight initialization-sliding window fusion convolutional neural network," complexity, vol. 2019, 2019.

[59] M. Maqsood, F. Nazir, U. Khan, F. Aadil, H. Jamal, I. Mehmood, et al., "Transfer learning assisted classification and detection of Alzheimer's disease stages using 3D MRI scans," Sensors, vol. 19, p. 2645, 2019.

[60] H. Acharya, R. Mehta, and D. K. Singh, "Alzheimer Disease Classification Using Transfer Learning," in 2021 5th International Conference on Computing Methodologies and Communication (ICCMC), 2021, pp. 1503-1508.

[61] R. A. Hazarika, D. Kandar, and A. K. Maji, "An experimental analysis of different deep learning based models for Alzheimer's disease classification using brain magnetic resonance images," Journal of King Saud University-Computer and Information Sciences, 2021.

[62] H. Wang, Y. Shen, S. Wang, T. Xiao, L. Deng, X. Wang, et al., "Ensemble of 3D densely connected convolutional network for diagnosis of mild cognitive impairment and Alzheimer's disease," Neurocomputing, vol. 333, pp. 145-156, 2019.

[63] S. Naz, A. Ashraf, and A. Zaib, "Transfer learning using freeze features for Alzheimer neurological disorder detection using ADNI dataset," Multimedia Systems, pp. 1-10, 2021.

[64] R. Pohle and K. D. Toennies, "Segmentation of medical images using adaptive region growing," in Medical Imaging 2001: Image Processing, 2001, pp. 1337-1346.

[65] J. Ashburner, "A fast diffeomorphic image registration algorithm," Neuroimage, vol. 38, pp. 95-113, 2007.

[66] D. Pan, A. Zeng, L. Jia, Y. Huang, T. Frizzell, and X. Song, "Early detection of Alzheimer's disease using magnetic resonance imaging: a novel approach combining convolutional neural networks and ensemble learning," Frontiers in neuroscience, vol. 14, p. 259, 2020.

[67] A. Laishram, & K. Thongam, "Automatic Classification of Oral Pathologies Using Orthopantomogram Radiography Images Based on Convolutional Neural Network," International Journal of Interactive Multimedia and Artificial Intelligence, vol. 7, no. 4, pp. 69-77, 2022.

[68] M. Rajesh, "Preprocessing and Skull Stripping of Brain Tumor Extraction from Magnetic Resonance Imaging Images Using Image Processing," Recent Trends in Intensive Computing, vol. 39, pp. 299 - 307, 2021.

[69] B. Perumal, J. Deny, S. Devi, & V. Muneeswaran, (2021, May). Region based Skull Eviction Techniques: An Experimental Review. In 2021 5th International Conference on Intelligent Computing and Control Systems (ICICCS) (pp. 629-634). IEEE.

[70] H.S.M. Chen, V. A. Kumar, J. M. Johnson, M. M. Chen, K. R. Noll, P. Hou, H. L. Liu, "Effect of brain normalization methods on the construction of functional connectomes from resting-state functional MRI in patients with gliomas," Magnetic resonance in medicine, vol. 86, no. 1, pp. 487-498, 2021.

[71] C. Salvatore, A. Cerasa, P. Battista, M. C. Gilardi, A. Quattrone, and I. Castiglioni, "Magnetic resonance imaging biomarkers for the early diagnosis of Alzheimer's disease: a machine learning approach," Frontiers in neuroscience, vol. 9, p. 307, 2015.

Muhammad Irfan

Muhammad is pursuing PhD degree in Information Technology at the Western Sydney University. His research interest includes artificial intelligence, machine learning and deep learning.

Seyed Shahrestani

Seyed completed his PhD degree in Electrical and Information Engineering at the University of Sydney. He joined Western Sydney University in 1999, where he is currently a Senior Lecturer. He is also the head of the Networking, Security and Cloud Research (NSCR) group at the University.

Mahmoud Elkhodr

Mahmoud is Lecturer at Central Queensland University (CQU) Sydney Campus. His main teaching and research interests include Internet of Things (IoT), Computer Networking, Mobile technologies, health ICT, Security, and Privacy.